Science Advances

AAAS

advances.sciencemag.org/cgi/content/full/4/3/eaap8492/DC1

Supplementary Materials for

Repopulating retinal microglia restore endogenous organization and function under CX3CL1-CX3CR1 regulation

Yikui Zhang, Lian Zhao, Xu Wang, Wenxin Ma, Adam Lazere, Hao-hua Qian, Jun Zhang, Mones Abu-Asab, Robert N. Fariss, Jerome E. Roger, Wai T. Wong

Published 21 March 2018, *Sci. Adv.* **4**, eaap8492 (2018)
DOI: 10.1126/sciadv.aap8492

The PDF file includes:

Other Supplementary Material for this manuscript includes the following:
(available at advances.sciencemag.org/cgi/content/full/4/3/eaap8492/DC1)

- movie S1 (.avi format). Dynamic migration and in situ replication of repopulating microglia in the retina.
- movie S2 (.avi format). Dynamic migration and replication of repopulating microglia slow down as microglial density increases in the retina.
- movie S3 (.avi format). Repopulating microglia demonstrate dynamic motility in their processes at baseline and in response to exogenous ATP that are similar to that in endogenous microglia.

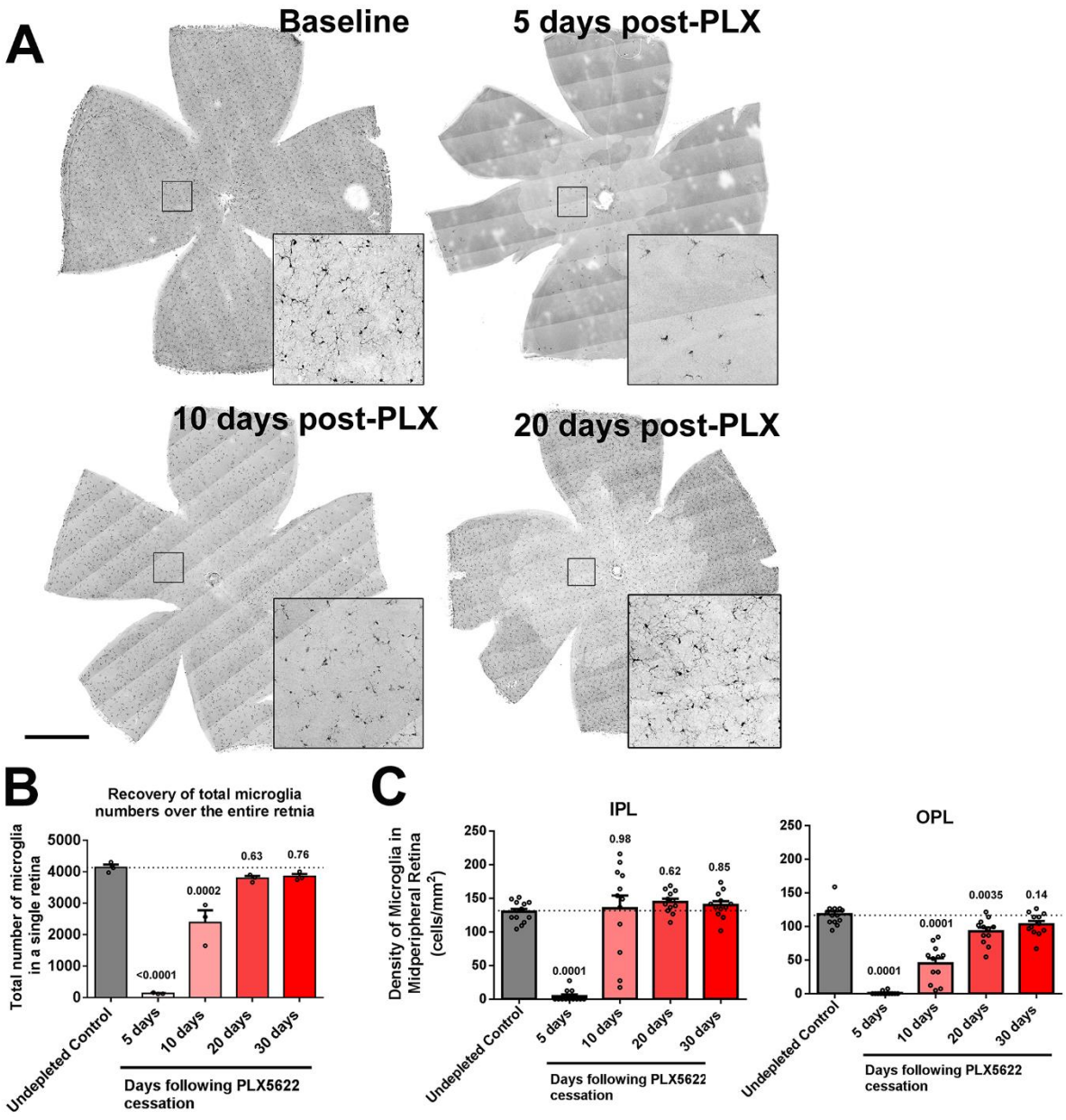
A
Baseline
5 days post-PLX
10 days post-PLX
20 days post-PLX
B
Recovery of total microglia numbers over the entire retnia
Total number of microglia in a single retina
5000
4000
3000
2000
1000
0
<0.0001
0.0002
0.63
0.76
Undepleted Control
5 days
10 days
20 days
30 days
Days following PLX5622 cessation
C
IPL
Density of Microglia in Midperipheral Retina (cells/mm²)
250
200
150
100
50
0
0.0001
0.98
0.62
0.85
Undepleted Control
5 days
10 days
20 days
30 days
Days following PLX5622 cessation
OPL
250
200
150
100
50
0
0.0001
0.0001
0.0035
0.14
Undepleted Control
5 days
10 days
20 days
30 days
Days following PLX5622 cessation

fig. S1. Microglial repopulation in the adult wild-type mouse retina in a pharmacological (PLX5622) model of microglial depletion demonstrates a center-to-peripheral, vitreal-to-scleral progression. (**A**) Depletion of retinal microglia was induced pharmacologically using PLX5622, a small-molecule inhibitor of the microglia-specific CSF1 receptor whose signaling is required for microglial survival. Young adult 8-12-week old wild type (C57Bl6) mice were maintained on regular chow supplemented with PLX5622 (1.2 mg/kg chow, ≈6mg/day) for a 7-day period to induce microglia depletion, followed by a return to regular chow (without PLX5622) to allow for microglial repopulation. Retina flat-mounts were prepared from undepleted controls at baseline and at 5, 10, and 20 days following PLX5622 cessation; insets show Iba1+ repopulating cells at higher magnification. Scale bar = 1mm. (**B**) The total number of Iba1+ cells in the retina was measured as a function of time following PLX5622 administration (1-way ANOVA, Sidak's multiple comparison test, n = 3 animals of mixed sex at each time point). (**C**) The density of repopulating cells in the IPL and OPL were separately determined at the same time points. Repopulation to baseline density levels occurred first in the IPL (by 10 days) and later in the OPL (by 20-30 days) 1-way ANOVA, Sidak's multiple comparison test, n = 12 imaging fields from 3 animals of mixed sex at each time point).

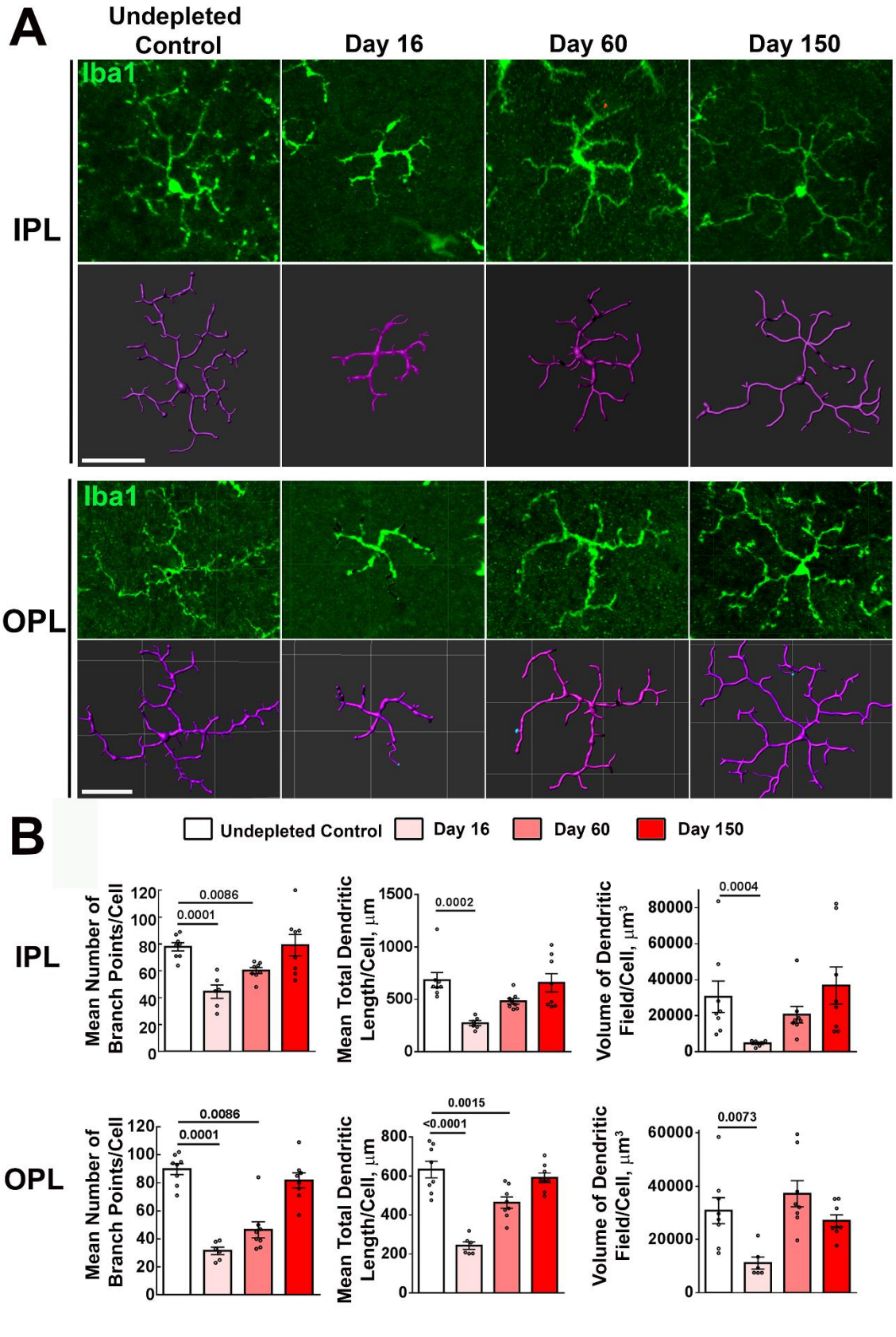
A
Undepleted Control
Day 16
Day 60
Day 150
IPL
Iba1
OPL
Iba1
B
Undepleted Control
Day 16
Day 60
Day 150
IPL
Mean Number of Branch Points/Cell
0.0086
0.0001
Mean Total Dendritic Length/Cell, µm
0.0002
Volume of Dendritic Field/Cell, µm³
0.0004
OPL
Mean Number of Branch Points/Cell
0.0086
0.0001
Mean Total Dendritic Length/Cell, µm
0.0015
<0.0001
Volume of Dendritic Field/Cell, µm³
0.0073

fig. S2. Repopulating Iba1^{+} cells undergo progressive morphological maturation to recapitulate morphologies of endogenous retinal microglia in the *CX3CR1^{CreER}*-DTA model of microglial depletion. (**A**) Morphologies of repopulating Iba1+ cells (*green*) were quantitatively analyzed prior to and at various times during repopulation (day 16, 60, 150) in the CX3CR1^{CreER}-DTA model using computer-assisted segmentation of microglial processes; 3D-rendering of individual cell morphologies are shown in purple. Repopulating cells in the IPL and OPL at day 16 had small dendritic arbors with few branches; these progressively increased with time to resemble morphologies observed in endogenous microglia. Scale bar = 40µm. (**B**) Morphological parameters of mean number of branch points per cell, mean total length of all processes per cell, and mean volume of the 3-dimensional envelope subtending all the process of a single cell were assessed, showing recovery of baseline parameters by day 150 (p values <0.05 are shown, from 1-way ANOVA with Dunn's multiple comparison test, n = 6 cells each from 3 mice at day 16, n=8 cells each from 3 mice at other time-points).

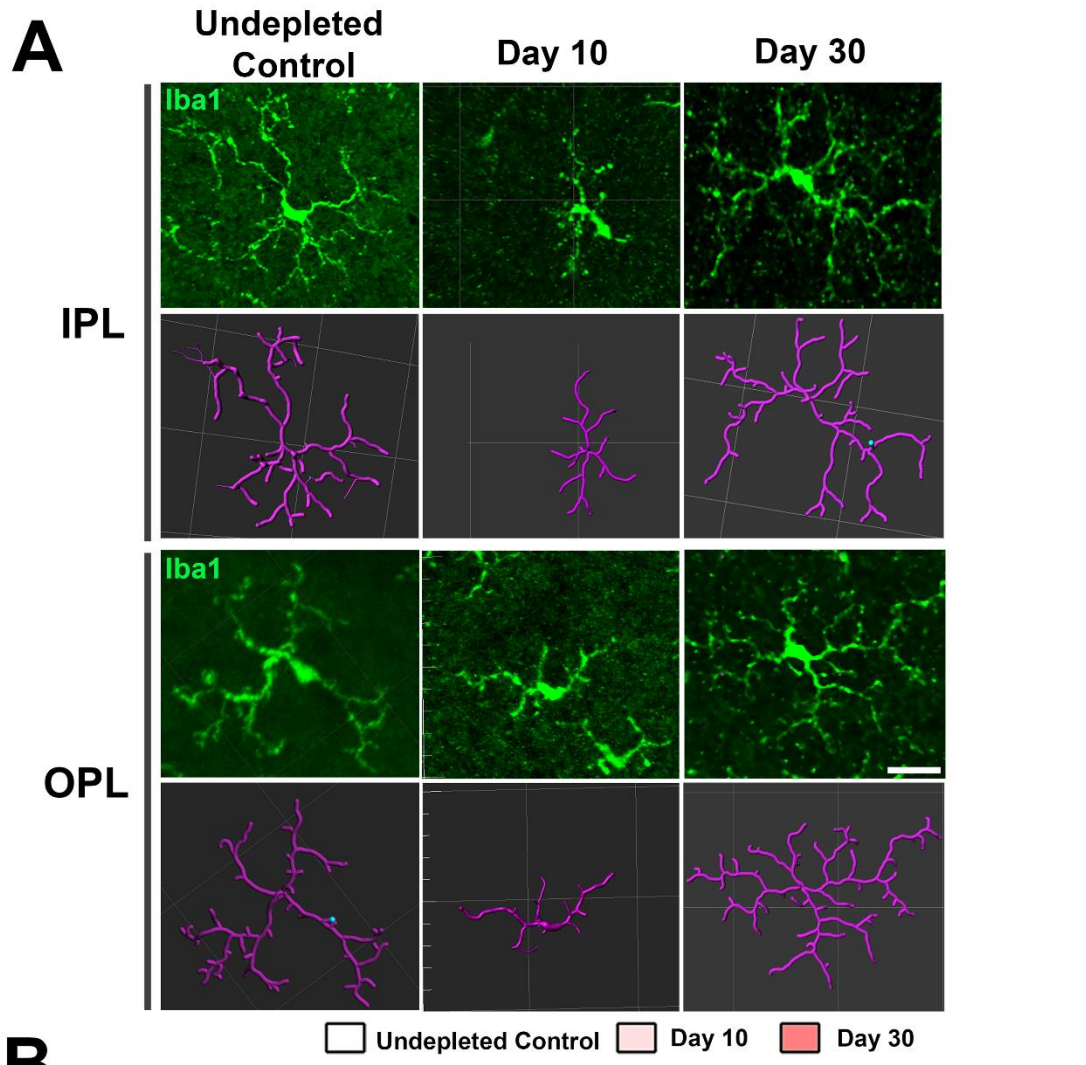
A
Undepleted Control
Day 10
Day 30
IPL
OPL
Iba1
Iba1

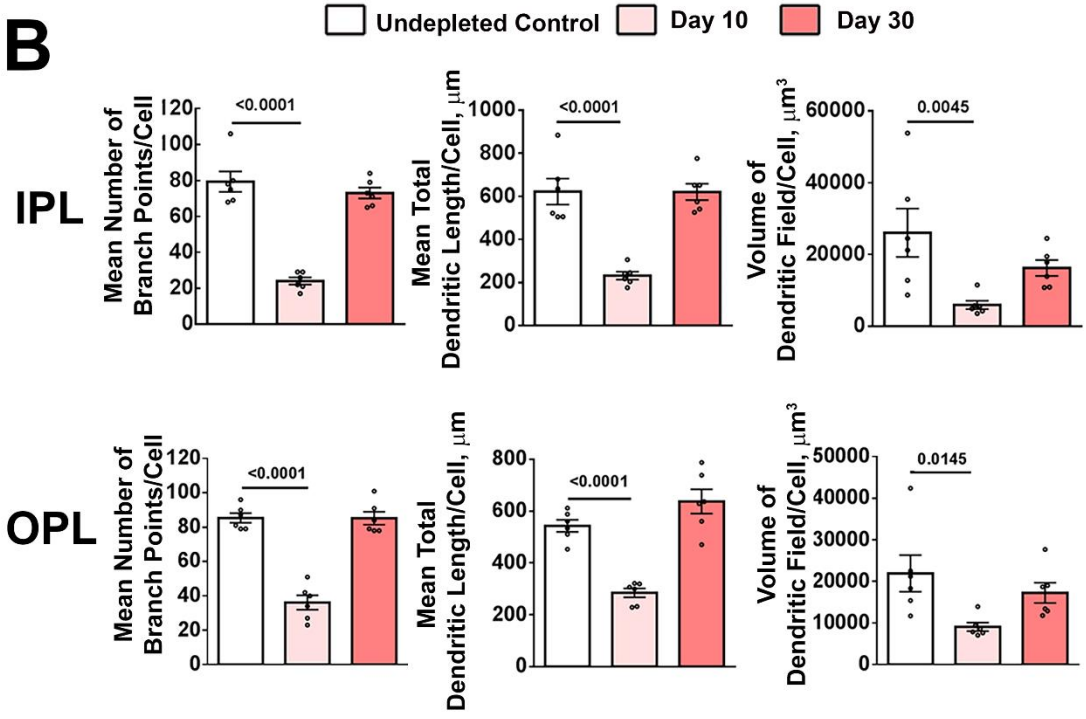
B
Undepleted Control
Day 10
Day 30
IPL
OPL
Mean Number of Branch Points/Cell
Mean Total Dendritic Length/Cell, µm
Volume of Dendritic Field/Cell, µm³
<0.0001
<0.0001
0.0045
<0.0001
<0.0001
0.0145

fig. S3. Repopulating Iba1^{+} cells undergo progressive morphological maturation to recapitulate morphologies of endogenous retinal microglia in the PLX5622-mediated model of microglial depletion. (**A**) Morphologies of repopulating Iba1+ cells were quantitatively analyzed prior to and at various times during repopulation (day 10 and day 30) following 7 days of PLX5622 administration to deplete retinal microglia. Individual Iba1+ cells in the IPL and the OPL were imaged with confocal microscopy and analyzed using Imaris software; 3D-rendering of individual cell morphologies are shown in purple. Scale bar = 20μm. (**B**) Iba1+ cells during early repopulation (day 10) possessed simple, small arbors that occupied small volumes. When repopulation neared completion (day 30), morphological parameters of microglia have increased to resemble those in the undepleted controls (1-way ANOVA with Dunn's multiple comparison test, n = 6 cells each from 3 mice at each time-point).

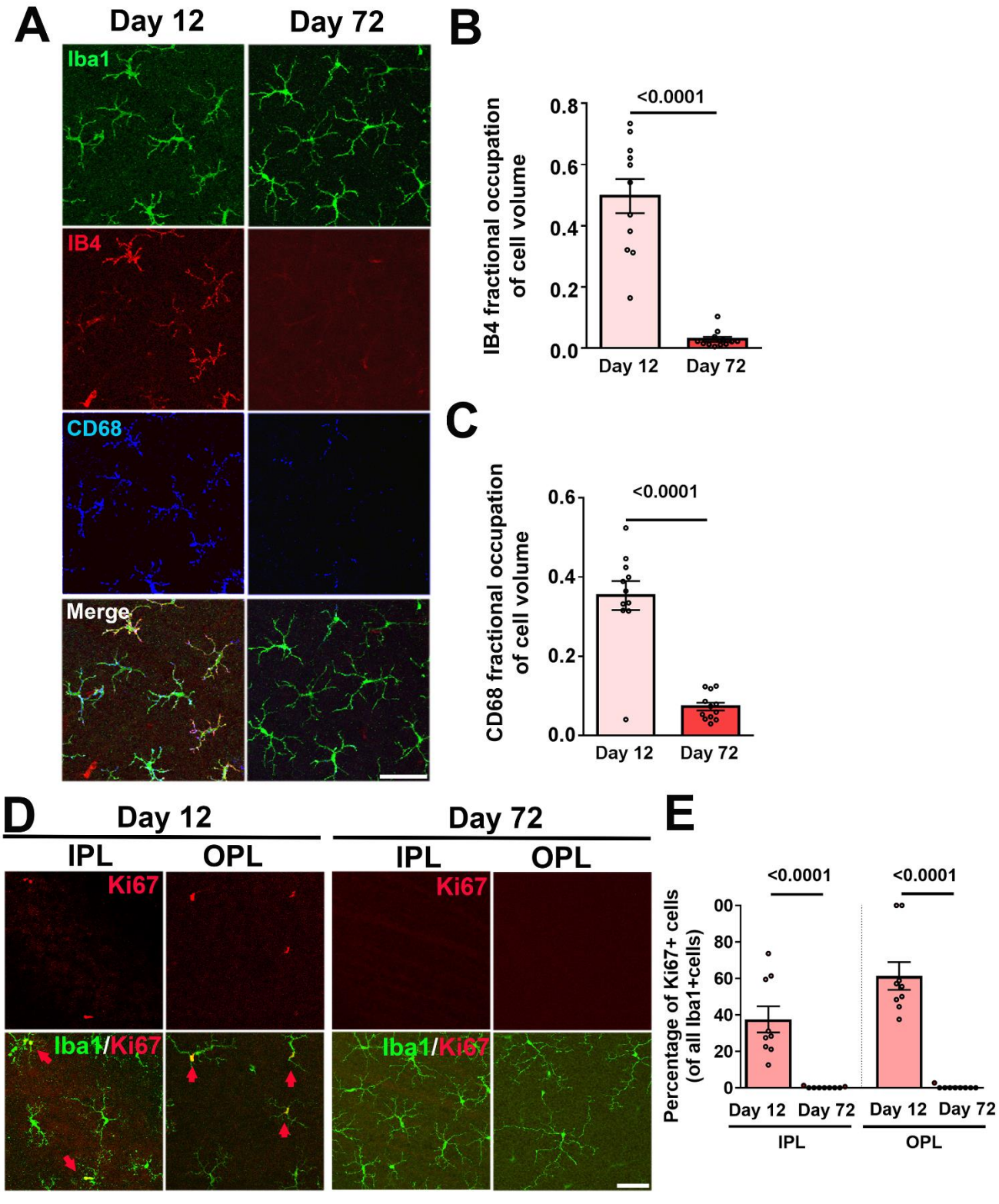
A
Day 12
Day 72
Iba1
IB4
CD68
Merge
B
IB4 fractional occupation of cell volume
<0.0001
0.8
0.6
0.4
0.2
0.0
Day 12
Day 72
C
CD68 fractional occupation of cell volume
<0.0001
0.6
0.4
0.2
0.0
Day 12
Day 72
D
Day 12
Day 72
IPL
OPL
IPL
OPL
Ki67
Ki67
Iba1/Ki67
Iba1/Ki67
E
Percentage of Ki67+ cells (of all Iba1+cells)
<0.0001
<0.0001
00
80
60
40
20
0
Day 12
Day 72
Day 12
Day 72
IPL
OPL

fig. S4. Repopulating Iba1^{+} cells demonstrate transient expression of markers of microglial activation and replication in the *CX3CR1^{CreER}*-DTA model of microglial depletion. (**A**) Repopulating Iba1+ demonstrated prominent cytoplasmic staining for microglial activation markers IB4 (*red*) and CD68 (*blue*) at day 12 following last tamoxifen administration, but these decreased markedly by day 72. Fractional cytoplasmic occupation of IB4 (**B**) and CD68 staining (**C**) demonstrated significant decreases from day 12 to 72 (p values from Mann-Whitney test, n = 11 and 12 cells from 3 animals at D12 and D72 respectively). Scale bar = 50 µm. (**D**) Proliferating Iba1+ cells were identified using Ki67 immunopositivity at day 12 and 72 (cells immunopositive for both Iba1 and Ki67 are indicated by *red arrows*). Scale bar = 50 µm. (**E**) The prevalence of Ki67+ cells among Iba1+ cells was high in both the IPL and OPL at day 12, but nearly undetectable at day 72 (Mann-Whitney test, n = 9 imaging fields in each age group).

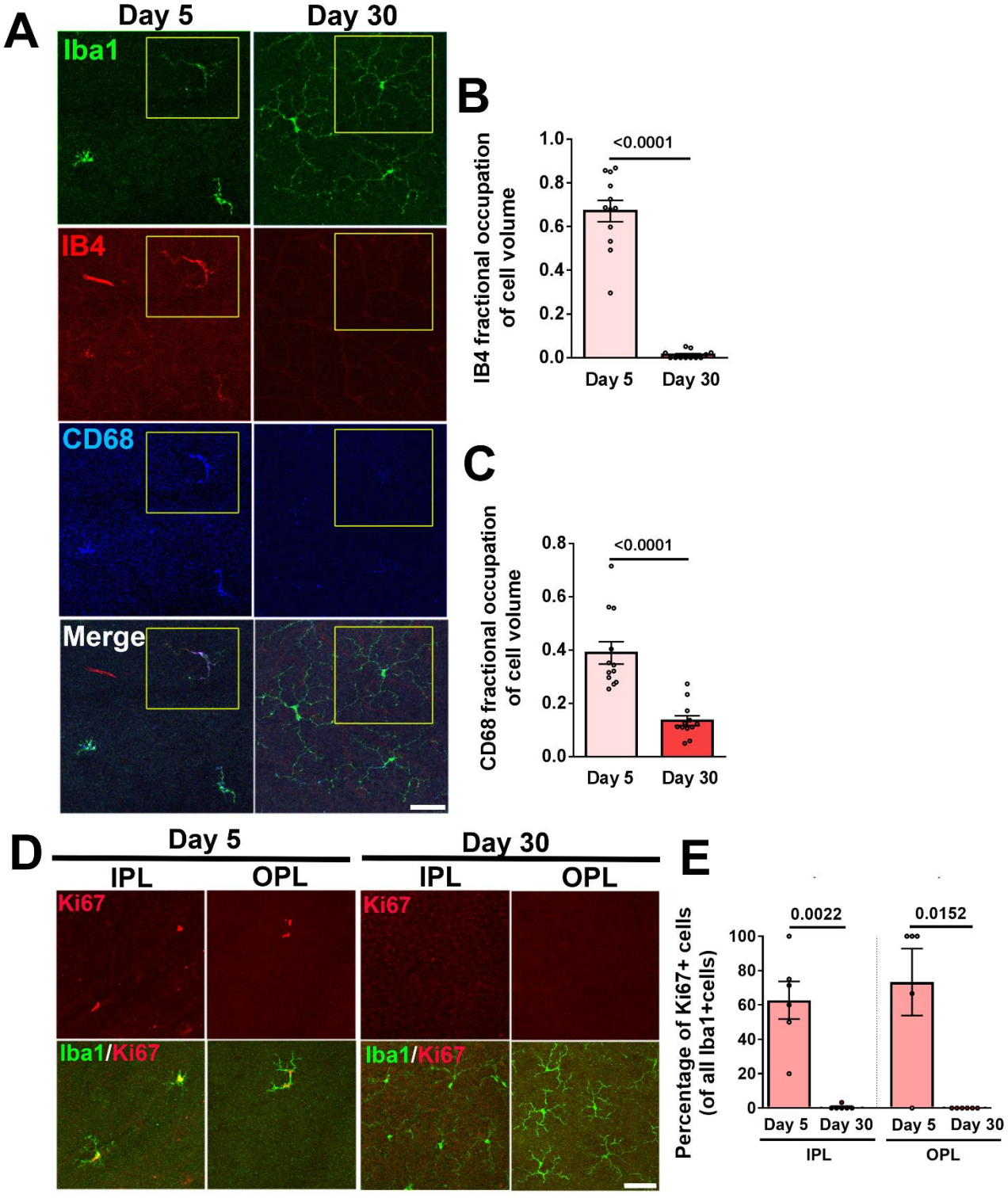
A
Day 5
Day 30
Iba1
IB4
CD68
Merge
B
IB4 fractional occupation of cell volume
<0.0001
1.0
0.8
0.6
0.4
0.2
0.0
Day 5
Day 30
C
CD68 fractional occupation of cell volume
<0.0001
0.8
0.6
0.4
0.2
0.0
Day 5
Day 30
D
Day 5
Day 30
IPL
OPL
IPL
OPL
Ki67
Iba1/Ki67
Ki67
Iba1/Ki67
E
Percentage of Ki67+ cells (of all Iba1+cells)
0.0022
0.0152
100
80
60
40
20
0
Day 5
Day 30
Day 5
Day 30
IPL
OPL

fig. S5. Repopulating Iba1^{+} cells demonstrate transient expression of markers of activation and replication in the PLX5622-induced model of microglial depletion. (**A**) Repopulating Iba1+ demonstrated prominent cytoplasmic staining for microglial activation markers IB4 (*red*) and CD68 (*blue*) at day 5 but staining was markedly decreased at day 30, when repopulation was fairly complete (typical examples of repopulating microglia at the two time-points are highlighted in the yellow boxes), as evidenced by significantly lower fractional occupation of cytoplasm by IB4 (**B**) and CD68 staining (**C**). (p values from Mann-Whitney test, n = 12 cells from 3 animals in each group). Scale bar = 50 µm. (**D**, **E**) The prevalence of cell division was followed with Ki67 immunolabeling; the prevalences of Ki67+ cells among Iba1+ cells were high in both the IPL and OPL at day 5, but nearly undetectable at day 30 when repopulation was nearing completion (Mann-Whitney test, n = 5-6 fields from 3 mice in each age group). Scale bar = 50 µm.

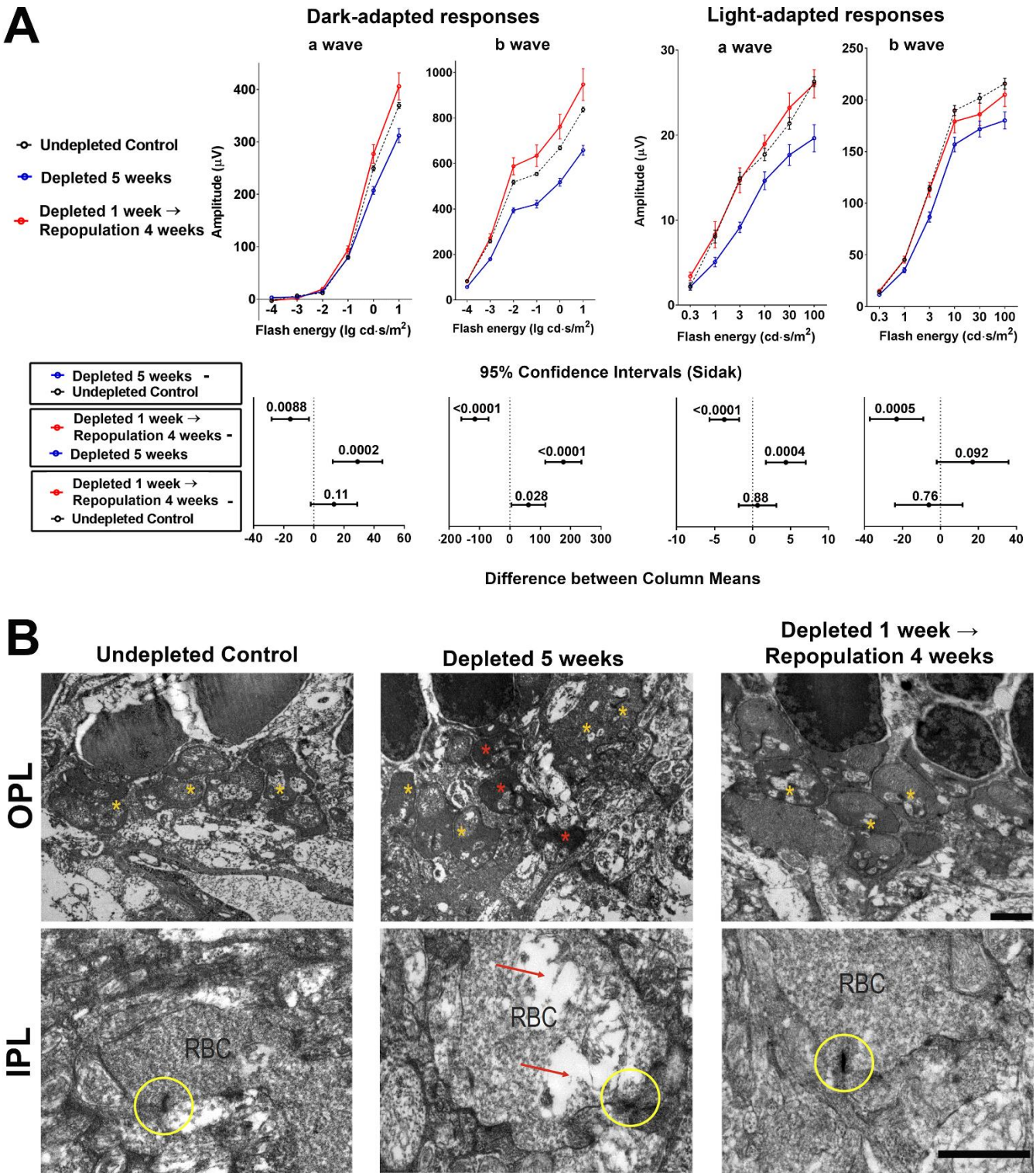
A
Dark-adapted responses
Light-adapted responses
a wave
b wave
a wave
b wave
Undepleted Control
Depleted 5 weeks
Depleted 1 week → Repopulation 4 weeks
Amplitude (μV)
Flash energy (lg cd·s/m²)
Flash energy (cd·s/m²)
95% Confidence Intervals (Sidak)
Depleted 5 weeks - Undepleted Control
Depleted 1 week → Repopulation 4 weeks - Depleted 5 weeks
Depleted 1 week → Repopulation 4 weeks - Undepleted Control
0.0088
0.0002
0.11
<0.0001
<0.0001
0.028
<0.0001
0.0004
0.88
0.0005
0.092
0.76
Difference between Column Means
B
Undepleted Control
Depleted 5 weeks
Depleted 1 week → Repopulation 4 weeks
OPL
IPL
RBC
RBC
RBC

fig. S6. Microglial repopulation rescues deterioration of retinal function induced by microglia depletion in the PLX5622 model. (**A**) Ten-week old wild type mice were subjected to transient PLX5622-induced microglia depletion for one week. Following this period, experimental mice were divided into two subgroups: (1) maintained microglial depletion for an additional 4 weeks (total 5 weeks depletion, *blue line*), (2) repopulation for 4 weeks (*red line*). Undepleted age-matched wild-type animals served as controls (*black dotted line*). Mice subjected to retinal microglial depletion for 5 weeks demonstrated in a general decrease in ERG responses, however mice allowed to undergo repopulation following acute depletion did not show comparable decreases, indicating that repopulating microglia were able to maintain functional ERG responses from deterioration. *Upper panels* show ERG amplitudes in all subgroups, data points and error bars indicate mean responses ± SEM. *Lower panels* show statistical comparisons between subgroups with data points and error bars indicating mean differences and ± 95% confidence limits (error bars not crossing x = 0 indicate significant ($p<0.05$) comparisons). Two-way ANOVA with Sidak's multiple comparison test was used to calculate p values; n = 30 eyes in 15 animals in control subgroup, 20 eyes in 10 animals in the depletion subgroup, 10 eyes in 5 animals for the repopulation subgroup. (**B**) (*Upper panels*) Electron microscopic analysis of the synaptic structures in retinas from the three experimental groups in (A) was performed. OPL synapses in undepleted controls demonstrated normal photoreceptor synaptic termini (*yellow **), but retinas depleted of microglia for 5 weeks showed an increased prevalence of synaptic termini with dystrophic, irregular morphology and increased osmiophilic cytoplasm (*red **), a feature not similarly observed in retinas that have undergone repopulation. (*Lower panels*) Analysis of synaptic termini of rod bipolar cells (RBC) in the IPL demonstrated structural disruptions (*red arrows*) and shortened ribbons (*yellow circles*) in the depleted 5 weeks group, while the termini in repopulated retinas resembled that of undepleted controls. Scale bars = 1 μm.

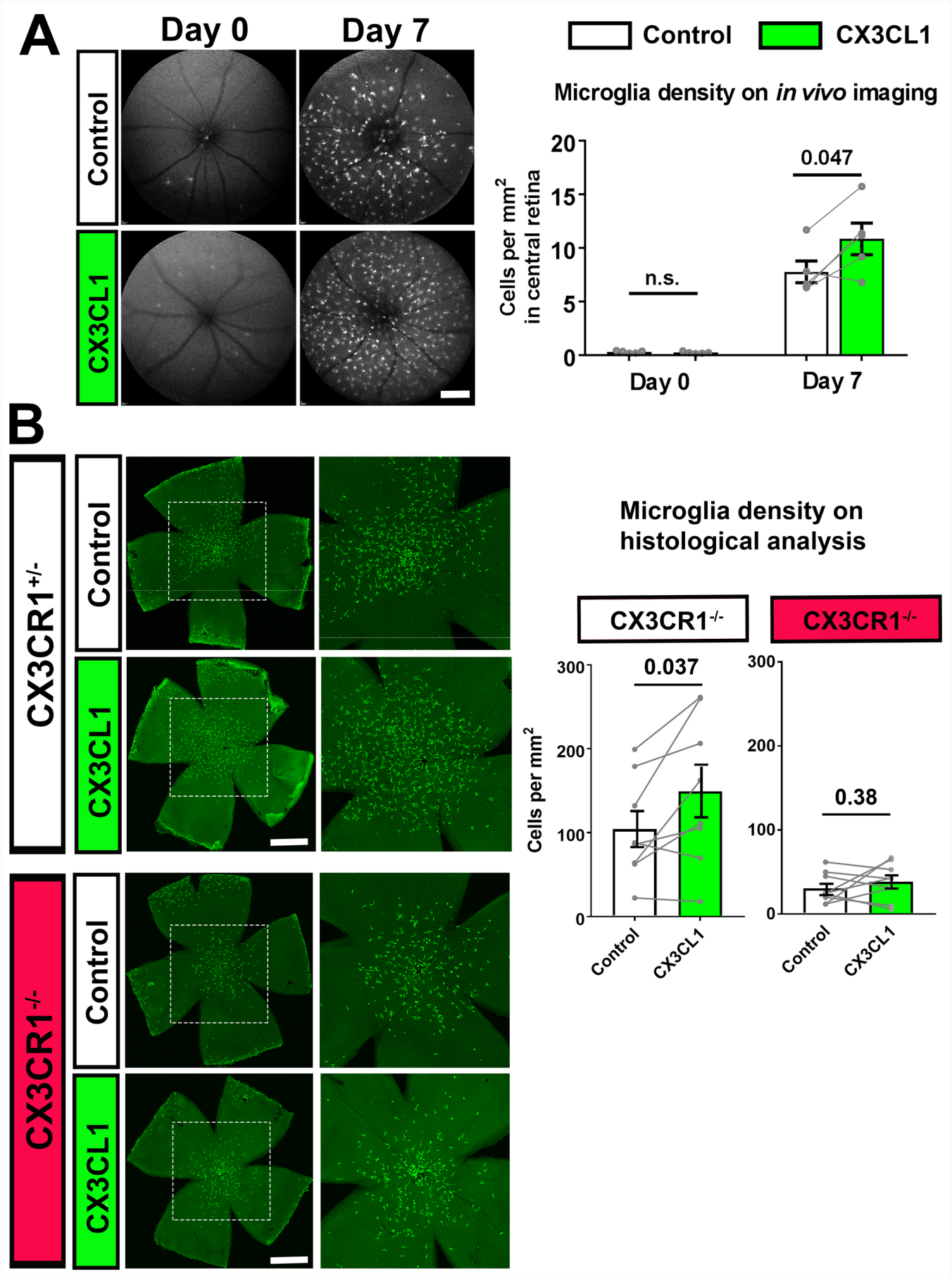
A
Day 0
Day 7
Control
CX3CL1
Control
CX3CL1
Microglia density on *in vivo* imaging
Cells per mm^2 in central retina
20
15
10
5
0
n.s.
0.047
Day 0
Day 7
B
CX3CR1$^{+/-}$
CX3CR1$^{-/-}$
Control
CX3CL1
Control
CX3CL1
Microglia density on histological analysis
CX3CR1$^{-/-}$
CX3CR1$^{-/-}$
Cells per mm^2
300
200
100
0
0.037
0.38
Control
CX3CL1
Control
CX3CL1

fig. S7. Intravitreal delivery of exogenous CX3CL1 accelerates microglial repopulation. *CX3CR1*$^{+/GFP}$ and *CX3CR1*$^{+/GFP}$ (CX3CR1 deficient) mice (2-3-month old) were subjected to PLX5622-mediated microglial depletion for 7 days and allowed to undergo microglial repopulation. On day 3 of the repopulation phase, recombinant CX3CL1 (99ng) was intravitreally injected into one eye of each experimental animal; the contralateral eye was injected with heat-inactivated CX3CL1 and served as a control. (**A**) Microglial repopulation in the central retina was followed for the first 7 days of repopulation using *in vivo* fundus imaging of GFP-labeled microglia in *CX3CR1*$^{+/GFP}$ mice. Fluorescence imaging of a representative experimental animal demonstrates near complete depletion at day 0 (immediately following cessation of PLX5622) in both eyes. Following unilateral CX3CL1 delivery at day 3, fundus imaging showed significantly greater numbers of repopulating cells in the CX3CL1-treated eye relative to contralateral control eyes at day 7 (paired t-test, n =10 eyes in 5 animals). (**B**) Microglial repopulation over the entire retina at day 7 was quantified by histological analysis in retinal flat-mounts, showing significantly more repopulating microglia in CX3CL1-treated eyes compared with control eyes in *CX3CR1*$^{+/GFP}$ mice (paired t-test, n =16 eyes in 8 animals). However, the same treatment of CX3CL1 in *CX3CR1*$^{GFP/GFP}$ mice did not influence the rate of repopulation (paired t-test, n =18 eyes in 9 animals). Scale bar in A = 250 µm, B = 1000 µm.

A

Microglial repopulation in the CX3CR1^{cre}-DTA model

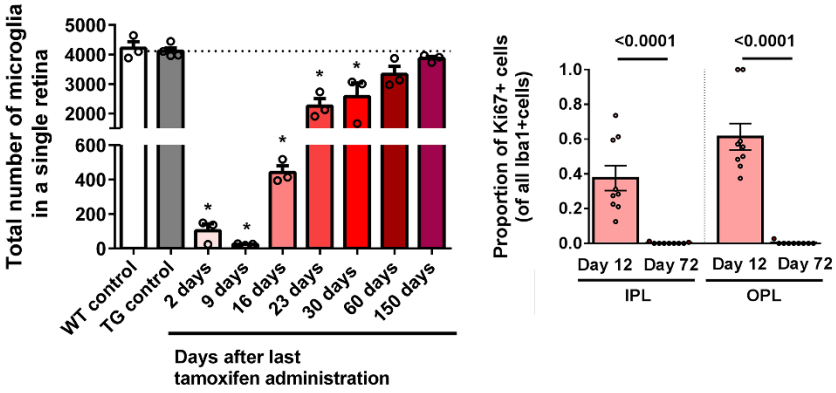

Assuming that 50% of cells were actively proliferating, the estimated doubling time in hours needed to achieve the changes in cell numbers:

Using the equation: $1.5^{(\text{Time interval/cell cycle duration})} = (\text{Cell \# at time 1/Cell \# at time 2})$

Day 9	→	Day 16	→	Day 23
24 cells		442 cells		2256 cells
Estimated time to complete one cell cycle:		23.4 hours		41.8 hours

B

Microglial repopulation in the PLX5622 model

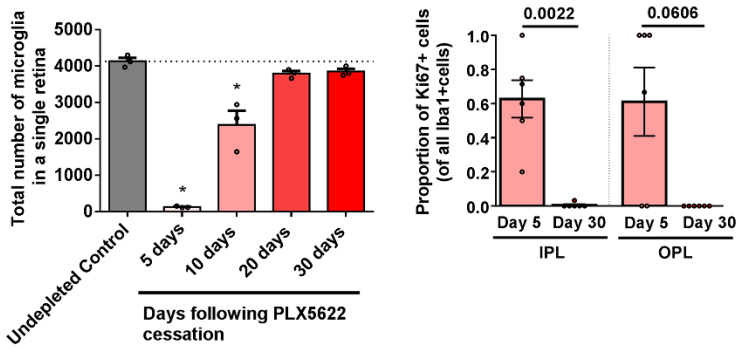

Assuming that 60% of cells were actively proliferating, the estimated doubling time in hours needed to achieve the changes in cell numbers:

Day 5	→	Day 10	→	Day 20
131 cells		2385 cells		3795 cells
Estimated time to complete one cell cycle:		19.4 hours		121.6 hours

Observations from in vivo imaging of microglial proliferation at Day 5 of repopulation in the PLX5622 model

Estimated rate of cell divisions: 0.0267 divisions/cell/hr = 0.64 divisions/cell/day

Estimated time to complete one cell cycle at day 5 of repopulation = 17.1 hours

fig. S8. Estimation of cell proliferation dynamics during the repopulation process: Proliferation rates of residual microglia are sufficient to regenerate cells observed during the repopulation process. (**A**) Following depletion in the *CX3CR1^{Cre}-DTA* model, the numbers of repopulating microglia in the entire retina were counted and plotted; the most rapid phase of proliferation occurred between 9 to 23 days following depletion. The proportion of proliferating cells as assessed by Ki67-labelling during this period was estimated to be 0.5. These numbers enable the estimated time to complete one cell cycle to be computed as 23.4 hours (between day 9 and 16) and 41.8 hours (between day 16 and 23). (**B**) Similar computations were performed for numbers obtained during repopulation following depletion in the PLX5622 model. The proportion of proliferating cells as assessed by Ki67-labelling during this period was estimated to be 0.6. These resulted in the estimated time to complete one cell cycle to be completed as 19.4 hours (between day 5 and 10) and 121.6 hours (between day 10 and 20). These estimated times to complete a cell cycle were in correspondence to the rates of cell division estimated from observations of cell proliferation obtained in *in vivo* imaging of the retina during repopulation in the PLX5622 model. In these calculations, the estimated time taken to complete one cell cycle at day 5 of repopulation was 17.1 hours, providing a lower bound for the estimations derived from cell counts. Together, these calculations indicate that extrapolating from *in vivo* observations of cell divisions, repopulating microglia numbers may reasonably be derived from *in situ* proliferation alone, without requiring an alternative source (e.g. from a progenitor pool) for repopulating cells.

LEGENDS TO SUPPLEMENTARY MOVIES

movie S1. Dynamic migration and in situ replication of repopulating microglia in the retina. Time-lapse movie of repopulating microglia in the central retina of a 11-week old *CX3CR1*$^{+/GFP}$ mouse at day 5 of the repopulation process (following 1 week of PLX5622 treatment) as captured with a scanning laser ophthalmoscope. All repopulating microglia in the field of view demonstrate dynamic migration in the horizontal plane of the retina with mean migration rates of ≈2 µm/min. Multiple microglia in the imaging field (*arrows*) demonstrate cellular division followed by the separation of the two daughter cells (*yellow circles*) by migration.

movie S2. Dynamic migration and replication of repopulating microglia slow down as microglial density increases in the retina. Time-lapse movie of repopulating microglia in the central retina of a 11-week old *CX3CR1*$^{+/GFP}$ mouse at day 12 of the repopulation process. Local microglial density has increased and migratory movements have become less marked with some cells showing stable soma positions. The prevalence of cellular divisions has also decreased compared with day 5 of the repopulation process.

movie S3. Repopulating microglia demonstrate dynamic motility in their processes at baseline and in response to exogenous ATP that are similar to that in endogenous microglia. Representative time-lapse movies obtained by *ex vivo* imaging in retinal explants from *CX3CR1*$^{+/GFP}$ mice of endogenous microglia (in undepleted animals) and repopulated microglia (60 days following PLX5622-mediated depletion). Repopulated microglia resembled endogenous microglia in (1) baseline motility of dynamic processes and (2) upregulation of process motility and elaboration of processes in responses to exogenous ATP application (1mM).